

Photocatalytic degradation of 2,4-dihydroxybenzoic acid in water: efficiency optimization and mechanistic investigations

Florence Benoit-Marquié ^a, Edith Puech-Costes ^a, André M. Braun ^b, Esther Oliveros ^{b,*},
Marie-Thérèse Maurette ^{a,*}

^a Laboratoire des IMRCP, Université Paul Sabatier, F-31062 Toulouse Cédex, France

^b Lehrstuhl für Umweltmesstechnik, Engler-Bunte-Institut, Universität Karlsruhe, D-76128 Karlsruhe, Germany

Abstract

The experimental design and response surface methodologies have been applied to the investigation of the TiO₂-photocatalytic degradation of 2,4-dihydroxybenzoic acid (DHBA) in aqueous solutions. It has been shown that a quadratic polynomial model may be used to assess adequately the efficiency of the photocatalytic degradation as a function of DHBA and TiO₂ concentrations. Moreover, the study of response surfaces leads to optimal conditions for investigating the catalyst efficiency. A degradation mechanism involving the cleavage of the DHBA aromatic ring at an early stage of the reaction is proposed. Such a mechanism accounts for the absence of any aromatic intermediate in the degradation process. © 1997 Elsevier Science S.A.

Keywords: 2,4-Dihydroxybenzoic acid; Experimental design; Modeling; Photocatalytic degradation; TiO₂

1. Introduction

In recent years, photochemical and photocatalytic oxidative degradation procedures (advanced oxidation processes) have been widely investigated for the treatment of contaminated waters and air [1–4]. In particular, the interest in semiconductor (mostly TiO₂) photocatalysis has been growing steadily, as it has been shown that this technique may be used to reduce the level of contamination due to a large variety of organic compounds.

Most of the investigations concerning the photocatalytic degradation of organic substances are carried out at low enough concentrations of contaminant in order to avoid competitive light absorption with the photocatalyst. Under these conditions, the initial rates of disappearance of the organic contaminant may be described by simple Langmuir–Hinshelwood kinetics (see, for example, Ref. [5]). However, among industrial waste waters, highly charged waters need to be treated which may contain e.g. aromatic substances at such concentrations that absorption tails of significant absorbance values extend into the UV-A region (320–380 nm) [6]. Therefore, we have been interested in investigating the effects of the concentrations of TiO₂ and 2,4-dihydroxybenzoic acid (DHBA), chosen as a model pollutant, on the degradation

rate of DHBA in aqueous solutions for concentration ranges in which competitive absorption occurs. It has been shown that DHBA is produced during the mineralization process of salicylic acid, which was earlier identified as a water pollutant [5]. DHBA is also formed by singlet oxygen and superoxide mediated oxidation of flavonoids [7], polyphenolic pigments widely present in plants. We have investigated the intermediates of the TiO₂-photocatalytic oxidation of DHBA and determined the influence of TiO₂ and DHBA concentrations on the degradation rate using the experimental design methodology [8–10] for modeling the reaction system. By following such a methodological approach, a statistically significant model may be obtained by performing a minimum set of well chosen experiments.

2. Experimental details

2.1. Materials

The photocatalyst powder used in this work was TiO₂ Degussa P25 (mainly anatase, surface area of approximately 50 m² g⁻¹). Particle size measurements by laser diffraction (Mastersizer X, Malvern Instruments SA) showed that aggregates of an average size of 4–5 µm are formed in aqueous suspensions, even under strong sonication. Therefore,

* Corresponding authors.

filtration with 0.45 μm Millipore discs (MF type) may be used for efficient removal of the suspended particles of TiO_2 . DHBA, 3,4-dihydroxybenzoic acid and 2,4,6-trihydroxybenzoic acid (Fluka, 98% purity), formic acid, glyoxalic acid and oxalic acid (Jansen, 99% purity) were used without further purification. All aqueous solutions were prepared with doubly distilled water.

2.2. Irradiation experiments

Irradiation was carried out in a DEMA (Mangels, Bornheim-Roisdorf, Germany) 13/12 *Solidex* glass annular reactor containing 250 cm^3 of solution. A medium pressure mercury lamp (Philips HPK 125 W) was positioned in the axis of the reactor (optical path 1.07 cm). The lamp stability was checked with a radiometer for the series of experiments included in the Doehlert uniform array (Section 2.4). Cooled water was circulated in the lamp jacket, maintaining a temperature of $20(\pm 0.5)^\circ\text{C}$ in the reaction mixture. The solution was magnetically stirred before and during irradiation, and permanently saturated with oxygen. The DHBA concentration was varied between 200 mg l^{-1} ($1.3 \times 10^{-3} \text{ mol l}^{-1}$) and 600 mg l^{-1} ($3.9 \times 10^{-3} \text{ mol l}^{-1}$), and that of TiO_2 between 1.75 and 4.25 g l^{-1} (Section 2.4).

2.3. Analyses

Samples of the reaction mixture were taken during irradiation, filtered through 0.45 μm Millipore discs and diluted for convenient analysis. Analysis was performed by high performance liquid chromatography (HPLC Waters 991, diode array detector, 250 nm, reverse phase column, length 25 cm, diameter 7 mm, packed with C18 μ Bondapack). The mobile phase was a mixture of 88% doubly distilled water, 10% acetonitrile (HPLC grade) and 2% acetic acid (RPE for analysis) (flow rate: 1.7 $\text{cm}^3 \text{ min}^{-1}$). Under these conditions, DHBA was eluted after 4.8 min. External calibration was performed for each series of experiments, a linear calibration curve relating the peak areas on the chromatograms and the DHBA concentrations. The HPLC analysis of the intermediates was carried out using a PRP-X300 Hamilton column (length 25 cm, diameter 4.1 mm) with an eluting mixture composed of methanol (HPLC grade) and $5 \times 10^{-2} \text{ mol l}^{-1} \text{ H}_2\text{SO}_4$ (RPE for analysis) in doubly distilled water (gradient: variation from 2 to 25% of methanol in 10 min, flow rate 1.3 $\text{cm}^3 \text{ min}^{-1}$). These conditions allowed separation of aliphatic acids, quinones, dihydroxybenzenes and aromatic acids with retention times of < 10 min, > 20 min, > 30 min and 35–50 min, respectively.

Absorption spectra were registered on a HP 8452 A spectrophotometer equipped with a diode array detector.

DHBA concentrations were determined by absorption spectrophotometry and HPLC. Both methods give similar results within experimental error.

Dissolved organic carbon (DOC) measurements were carried out using a DOC analyzer (DC 190, Dohrman) equipped with a non-dispersive infrared detector.

2.4. Experimental design

The experimental design methodology [8,9] provides a means of building a statistically significant model of a phenomenon by performing a minimum set of well chosen experiments. The experimental strategy is based on multivariate methods, and a large number of classical experimental designs adapted to various types of problems are available [8–13]. Data collection is more efficient and statistical data treatment easier than when using a technique consisting of changing the level (setting or value) of one input variable (controlled by the experimenter) at a time, while maintaining the other variables at fixed levels. Optimal experimental design is especially useful in the case where the effect of a given variable depends on the setting of another one and vice versa (interaction effects). Besides evaluation of the effects of different variables, modeling of the experimental response(s) of interest (e.g. degradation rate) is possible. The mathematical model is usually empirical (e.g. polynomials), as the mechanisms involved in the process investigated are usually complex and not completely understood. The resulting model allows the drawing of contour plots (lines or curves of constant response value) and, once tested, the prediction of the values of the response(s) at any point in the experimental region of interest (response surface methodology [10,11]). In summary, experimental design allows quantitative evaluation of the effects of different variables on responses of interest, quantitative evaluation of interaction effects between variables, comparison of these effects since variables are coded (without dimension, see below) and the possibility of minimizing the number of experiments relative to the information required, the experiments carried out being statistically the most significant.

This methodology has been used to the study of the influence of the concentration of TiO_2 and the initial DHBA concentration on the DHBA degradation rate (experimental response). In a previous study [6], the efficiency of the photocatalyzed oxidative degradation of pollutants contained in heavily contaminated industrial water was investigated using a pilot photochemical reactor. It was shown that a linear model, which was associated with the experimental design (complete factorial design at two levels), was not adequate for representing the response in the experimental region. Therefore, a Doehlert uniform array [12] has been chosen, which allows modeling of curved response surfaces. The associated response function (Y) is represented by a quadratic polynomial model:

$$Y = b_0 + \sum_{i=1}^k b_i X_i + \sum_{i=1}^k b_{ii} X_i^2 + \sum_{i=1}^{k-1} \sum_{j=2}^k b_{ij} X_i X_j \quad (1)$$

where $j > i$, k is the number of variables studied, b_0 is the average value of the experimental responses, b_i is the main

Table 1

Experimental matrix in coded and natural variables (Section 2.4) and corresponding experimental response, k_{ap} (Eq. (7)) for the Doehlert uniform array

Experiment no.	X_1	X_2	U_1 [DHBA] (mg l ⁻¹)	U_2 [TiO ₂] (g l ⁻¹)	k_{ap} ^a (mg ^{0.5} l ^{-0.5} min ⁻¹)	$k_{ap,cal}$ ^b (mg ^{0.5} l ^{-0.5} min ⁻¹)
1	1.0	0.0	594	3.00	0.122	0.128
2	-1.0	0.0	210	3.00	0.333	0.327
3	0.5	0.866	498	4.25	0.147	0.141
4	-0.5	-0.866	306	1.75	0.204	0.201
5	0.5	-0.866	498	1.75	0.122	0.116
6	-0.5	0.866	306	4.25	0.248	0.254
7	0.0	0.0	402	3.00	0.175	0.175
8	0.0	0.0	402	3.00	0.176	0.175
9	-0.27	-0.69	350	2.00	0.173	0.181

^a Standard deviation: $\pm 8\%$.^b Calculated with the quadratic polynomial model (Eq. (8)).

effect of the coded variable X_i , b_{ii} is the quadratic effect of the coded variable X_i , and b_{ij} is the first-order interaction effect between the coded variables X_i and X_j .

Since different variables are usually expressed in different units and/or have different limits of variation, their effects can only be compared if they are coded. Therefore, a reduced and centered variable X_i is associated with each natural variable U_i :

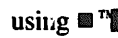
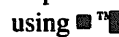
$$X_i = \frac{U_i - U_{i0}}{\Delta U_i} \quad (2)$$

where U_{i0} is the value of U_i at the center of the experimental region ($= (U_{i,max} + U_{i,min})/2$), and ΔU_i the step ($= (U_{i,max} - U_{i,min})/2$).

The range of variation of the natural variables determines the experimental region of interest. It was of interest to investigate the degradation of DHBA at concentrations higher than 10^{-3} mol l⁻¹. The concentration ranges of TiO₂ and DHBA (Section 2.2 and Table 1) were chosen from preliminary experiments with two objectives: to achieve DHBA degradation in less than 6 h and to avoid adsorption of more than 10% of DHBA onto the non-irradiated TiO₂ surface. Maximum adsorption was observed in the case of experiment nos. 3 and 6 (highest TiO₂ concentration, Table 1) with values of 10.1% and 10.5%. Adsorption-desorption equilibrium was reached within a few minutes.

The number of experiments to be carried out for a Doehlert uniform array is equal to $(k^2 + k + 1)$, where k is the number of variables studied. The experimental matrix for two variables (seven experiments) is given in Table 1, together with the corresponding values of the natural variables for the present study. The experimental points are uniformly distributed and can be represented as the apexes and center of a hexagon. Experiment no. 7 (center of the experimental domain) was repeated in order to check the reproducibility. All experiments were carried out under exactly the same conditions, except for the DHBA and TiO₂ concentrations (selected variables).

The least-squares estimates of the coefficients of Eq. (1) have been calculated from the values of the chosen experi-

mental response (k_{ap} , Section 3.2) in experiment nos. 1–7, using  software [13]. The regression significance and the model fit were assessed by F-testing. Drawings of the response surfaces and contour plots were also carried out using  software.

3. Results and discussion

3.1. Identification of intermediates and mechanism

The photocatalytic degradation of DHBA (200–600 mg l⁻¹) as a function of irradiation time in the presence of various quantities of TiO₂ (1.75–4.25 g l⁻¹) has been followed by HPLC and absorption spectrophotometry (Section 2.2 and Section 2.3). Control experiments have been performed in the absence of TiO₂ with the various DHBA initial concentrations as used for the Doehlert mixture. At all concentrations, 99% of the incident photons between 240 nm and 310 nm are absorbed on 1 cm or less. However, although DHBA absorbs part of the incident radiation (Solidex glass cuts off radiation at wavelengths lower than 285 nm), the degradation rate is considerably reduced in the absence of TiO₂. For example, more than 80% of an initial DHBA concentration of 498 mg l⁻¹ was degraded after 180 min in the presence of 4.25 g of TiO₂, whereas only 10% was removed by photolysis within the same period of irradiation (Fig. 1). In fact, photolysis leads to very similar results for the different concentrations investigated. Therefore, it is concluded that, in the presence of TiO₂, the dominant reaction is the photocatalytic degradation of DHBA, TiO₂ being in any case the only substance to absorb the 366 nm emission of the Hg arc.

The HPLC chromatograms obtained with the reverse phase column show that a degradation product with an absorption maximum at a wavelength of 210 nm is formed at the earliest stage of the reaction. Analysis of the absorption spectra of the aqueous solution at different irradiation times reveals that the absorbances (A) at the two absorption maxima of DHBA (250 nm and 292 nm) decrease with the same rate, the corresponding values of A/A_0 being identical within experimen-

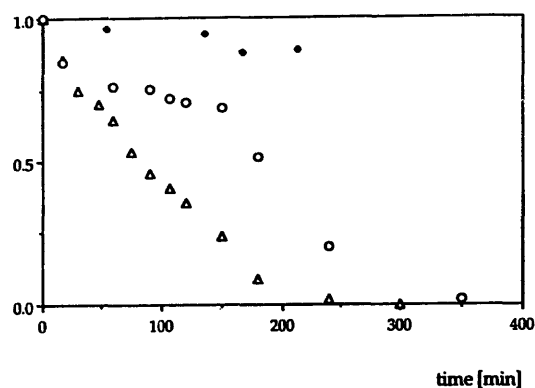


Fig. 1. Relative DHBA concentration (Δ) and relative DOC values (\circ) ($[\text{DHBA}] = 498 \text{ mg l}^{-1}$, $[\text{TiO}_2] = 4.25 \text{ g l}^{-1}$), and relative DHBA concentration in the absence of TiO_2 (\blacklozenge) as a function of irradiation time.

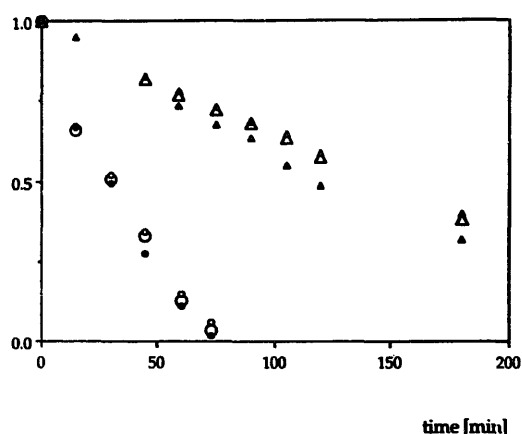
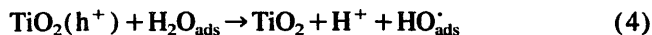


Fig. 2. Relative absorbance evolution at 250 nm and 292 nm as a function of irradiation time for experiment no. 1 (250 nm, Δ ; 292 nm, \blacktriangle) and experiment no. 2 (250 nm, \circ ; 292 nm, \circ) and corresponding decrease in relative DHBA concentrations determined by HPLC (no 1, \blacktriangle ; no. 3, \bullet).

tal error (Fig. 2 shows the cases of the fastest (no. 2) and slowest experiment (no. 1)). Moreover, the relative decrease in DHBA concentration determined by HPLC is only slightly faster than the decrease of corresponding relative absorbances. Therefore, no (or only negligible amounts of) aromatic intermediates are formed during the degradation process. This result has been confirmed by HPLC analysis using a PRP-X300 Hamilton column (Section 2.3): no aromatic acids, hydroxybenzenes, dihydroxybenzenes or quinonic compounds could be detected in the reaction mixture during irradiation. However, two aliphatic acids have been identified: oxalic acid (retention time: 1.9 min) as the main product and glyoxalic acid (retention time: 1.75 min) in much lower concentrations. Co-injection of the two acids with the reaction solution, as well as of mixtures including formic acid (retention time: 2.9 min), has been used for comparison and identification of the compounds. The absorption spectra of all the compounds have also been registered.

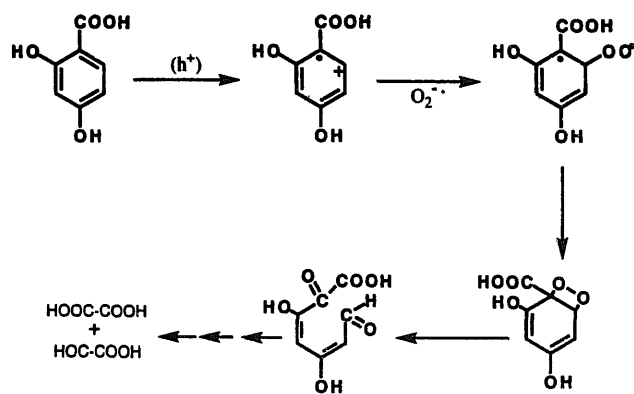
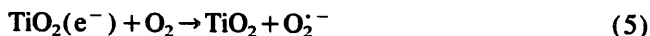
Previously published results [14–19] indicate that the first step of the degradation of aromatic compounds by photocatalysis is most often the formation of hydroxylated derivatives. The authors conclude that hydroxyl radicals (HO^\bullet),

formed by oxidation of adsorbed water molecules (Eqs. (3) and (4)), play a dominant role in the reaction.



This is the case, for example, in the TiO_2 -photocatalytic oxidation of salicylic acid where a mixture of hydroxylated aromatic isomers, including 2,4-dihydroxybenzoic acid, has been detected [5]. Catechol was also found, albeit in minor amounts, but, interestingly, no other stable aromatic intermediate which could arise from further degradation of these intermediates was mentioned by the authors. Moreover, it has been reported by Matthews [20] that “hydroxylation of the aromatic ring to give salicylic acid is a minor reaction path in the destruction of benzoic acid”. Taking into account electronic and steric factors, hydroxylation of DHBA would lead to the formation of 2,4,6-trihydroxybenzoic acid which could not be detected in the reaction mixture. Furthermore, we have checked that the photocatalytic degradation of 2,4,6-trihydroxybenzoic acid under the same conditions did yield aromatic and quinoid intermediates: their absorption spectra interfere with that of DHBA and, consequently, the absorbance at 292 nm increases, whereas the absorbance at 250 nm decreases during irradiation. Recently, different authors have shown that aromatic derivatives could also be oxidized directly by the holes at the TiO_2 surface, leading to the formation of quinoid compounds [16,21,22]. None of the intermediates mentioned above has been found in the case of DHBA.

These results lead to the conclusion that in the case of DHBA the opening of the aromatic ring occurs at a very early stage of the degradation process. A mechanism as represented in Scheme 1 may be proposed: hole (h^+) oxidation of the substrate leads to the formation of a radical cation, whereas the superoxide anion is formed by electron transfer from the conduction band of the photocatalyst to molecular oxygen (Eq. (5)); subsequent addition of superoxide to the radical cation of the aromatic substrate yields an unstable dioxetane, which leads to ring opening and formation of aliphatic acids.



Scheme 1. Possible mechanism for the TiO_2 -photocatalytic degradation of DHBA.

Another possible interpretation, similar to that proposed by Heller et al. [23], involves trapping of the initial radical cation by molecular oxygen, the intermediate peroxy radical reacting with the superoxide anion to yield an unstable tetroxide.

2,4- and 3,4-dihydroxybenzoic acids behave very similarly, as far as reaction rates and the absence of aromatic or quinoid intermediates are concerned, whereas the degradation of 2,4,6-trihydroxybenzoic acid proceeds by a different mechanism. It seems, therefore, that the ortho position with respect to the carboxylic group plays a key role in early ring opening, and that, following the mechanism proposed in Scheme 1, hole oxidation is favored at this position when unsubstituted (most probably for steric reasons).

DOC removal closely follows DHBA disappearance at the beginning of the degradation process, but some aliphatic intermediates (among them oxalic acid) are more difficult to eliminate, leading to a plateau in the DOC curve (Fig. 1). However, almost complete mineralization is observed soon after DHBA has been eliminated.

3.2. Experimental design

The photocatalytic degradation of DHBA as a function of irradiation time under the different experimental conditions of the Doehlert uniform array (Table 1) could not be fitted to a simple apparent kinetic order (pseudo-zero [24] or first order [20]), as observed previously for other aromatic compounds [25,26]. In most of these previous studies, the initial degradation rate of the organic substrate follows a Langmuir–Hinshelwood type kinetic model (see, for example, Refs. [5] and [16]). In fact, a rigorous kinetic approach has shown that the observed disappearance of the substrate follows kinetics of different orders, depending on the experimental conditions (especially the catalyst and substrate concentrations) [27]. Moreover, an analytical solution is only possible in some limiting cases, and the experimental error may lead

to confusion of a rather complex dependence with a simple one [27]. The purpose of this investigation is to establish an empirical model for evaluating the effects of catalyst and substrate initial concentrations on the global degradation efficiency of DHBA, and, hence, a rigorous kinetic model was not required. However, an experimental response adequately representing this efficiency had to be chosen. Under these experimental conditions, with relatively high TiO_2 and substrate concentrations, the best fits for the disappearance of DHBA as a function of irradiation time were obtained using an apparent order of 0.5 for the DHBA concentration:

$$[\text{DHBA}]/dt = -k_{\text{ap}}[\text{DHBA}]^{0.5} \quad (6)$$

and by integration

$$[\text{DHBA}]^{0.5} = [\text{DHBA}]_0^{0.5} - (k_{\text{ap}}/2)t \quad (7)$$

where $[\text{DHBA}]_0$ is the initial concentration of DHBA, and k_{ap} is the apparent rate constant for the disappearance of DHBA.

As shown in Fig. 3, plots of $([\text{DHBA}]/[\text{DHBA}]_0)^{0.5}$ versus time are linear. The values of k_{ap} have been calculated from the slopes of these plots and chosen as the experimental response representing the efficiency of DHBA degradation (Table 1).

The coefficients of the polynomial quadratic model (b_0, b_i, b_{ii}, b_{ij} , Eq. (1), Section 2.4) for the experimental response k_{ap} have been calculated by the least-squares method (regression analysis) [13] and are given in Eq. (8).

$$\begin{aligned} k_{\text{ap}} &= b_0 + b_1X_1 + b_2X_2 + b_{11}X_1^2 + b_{22}X_2^2 + b_{12}X_1X_2 \\ &= 0.175 - 0.099X_1 + 0.022X_2 + 0.052X_1^2 \\ &\quad - 0.013X_2^2 - 0.016X_1X_2 \end{aligned} \quad (8)$$

Variance analysis shows that the regression is significant and the postulated model represents well the phenomenon in the experimental region investigated: values of k_{ap} calculated with the model are in good agreement with experimental

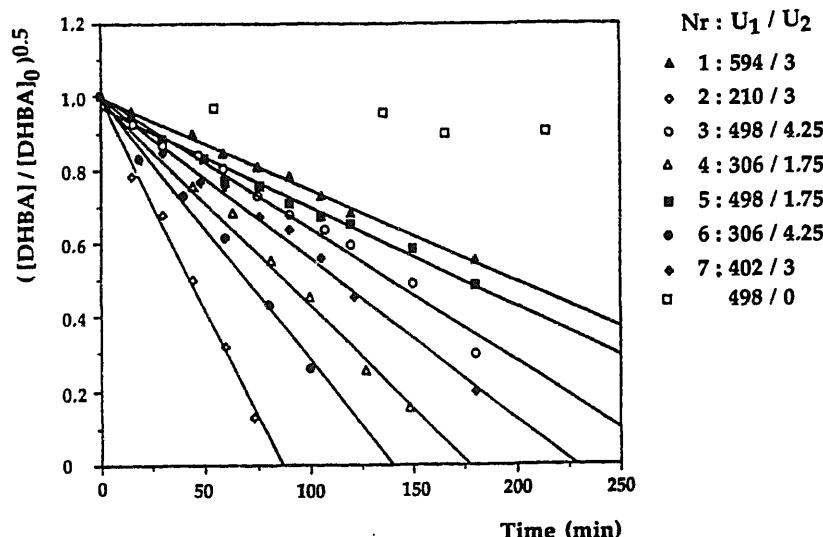


Fig. 3. Plots of $([\text{DHBA}]/[\text{DHBA}]_0)^{0.5}$ as a function of irradiation time for the series of experiments of the Doehlert uniform array (Eq. (7)). (The numbering of the experiments is the same as in Table 1; ratios (U_1/U_2) represent $[\text{DHBA}]/[\text{TiO}_2]$).

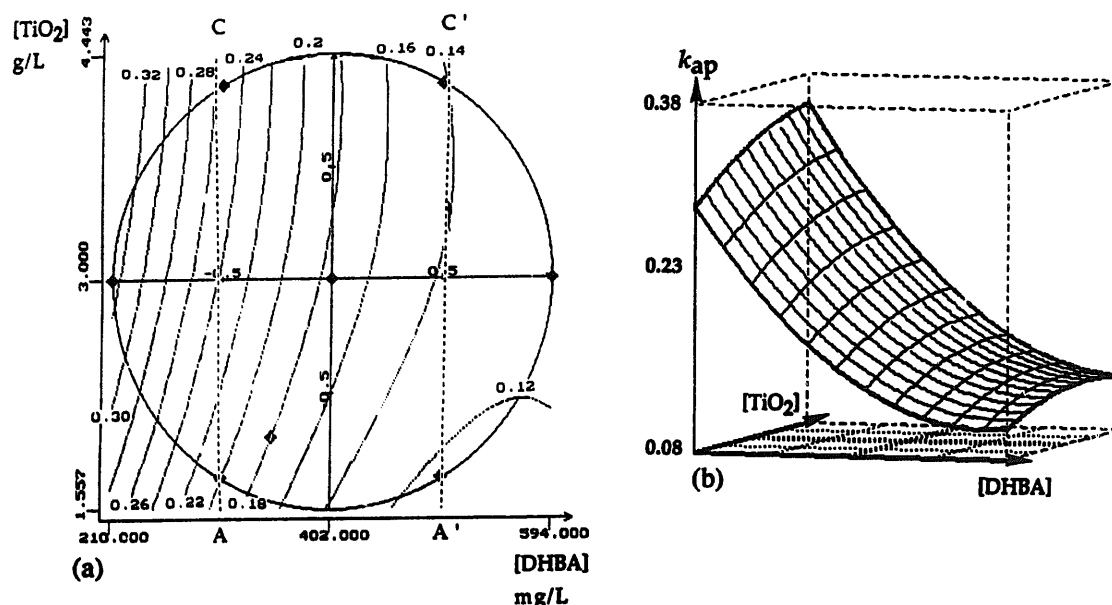


Fig. 4. Contour plot (a) and response surface (b) for the predicted value of the apparent rate constant of DHBA degradation, k_{ap} (experimental points of the Doehlert array (nos. 1–8) and the test point (no. 9) are indicated by \diamond).

values, for the experiments used to estimate the coefficients (nos. 1–8) as well as the control experiment (no. 9) (Table 1).

The contour plot (curves of constant response) and the three-dimensional response surface for k_{ap} are represented in Fig. 4.

In the range of concentrations investigated, the influence of $[DHBA]_0$ is more important than that of the concentration of TiO_2 . Whatever this concentration, the decrease of k_{ap} as $[DHBA]_0$ increases, follows a similar pattern: an almost linear decrease as long as $[DHBA]_0$ is lower than 402 mg l⁻¹ (center) and a flattening out of the response surface when $[DHBA]_0$ approaches the upper limit of the experimental region (594 mg l⁻¹). The decrease is faster at lower TiO_2 concentrations.

In the DHBA concentration range below 500 mg l⁻¹, an increase in TiO_2 concentration from its minimum to its maximum value (e.g. AC, Fig. 4a) leads to an increase in k_{ap} (about 30%). At higher DHBA concentrations, the photocatalyst concentration has almost no effect on the degradation efficiency (e.g. A'C', Fig. 4a). At high TiO_2 concentrations, the constant response curves become parallel with the $[TiO_2]$ axis (Fig. 4a), i.e. a plateau is reached for the degradation efficiency so that no benefit is obtained by increasing the TiO_2 concentration above 3.5 g l⁻¹. These observations are in agreement with previously published results. Different authors [6,18,28–31] have shown that the degradation rate generally increases with catalyst concentration until a plateau is reached. This plateau is generally explained by the maximum absorption of the incident light by the catalyst. In fact, most of the range of TiO_2 concentrations investigated in this work corresponds to the plateau region, hence the overall relative small effect of this variable.

4. Conclusion


By applying the experimental design methodology, we have shown that a quadratic polynomial model may be used to represent adequately the efficiency of the TiO_2 – photocatalytic degradation of DHBA in aqueous solutions in a concentration range of 200–600 mg l⁻¹. This model was established by performing a minimum of well-chosen experiments. This same methodology will be used for testing various TiO_2 samples (pure or on support) which we are currently preparing. Concerning the mechanism of the photocatalytic degradation of DHBA, we have proposed the cleavage of the aromatic ring as the first step of the reaction. Such a mechanism accounts for the absence of any aromatic or quinoid intermediates during the degradation process.

Acknowledgements

The authors gratefully acknowledge financial support of this work by the "Conseil Régional de Midi-Pyrénées". F.B.-M. thanks ADEME (Agence pour le Développement et la Maîtrise de l'Energie) for a grant. The authors also thank Professor A. Savall for his help in solving analytical problems.

References

- [1] N. Serpone and E. Pelizzetti (Eds.), *Photocatalysis, Fundamentals and Applications*, Wiley, New York, 1989.
- [2] O. Legrini, E. Oliveros and A.M. Braun, *Chem. Rev.*, 93 (1993) 671–698.
- [3] D.F. Ollis and H. Al-Ekabi (Eds.), *Photocatalytic Purification and Treatment of Water and Air*, Elsevier Science, Amsterdam, 1993.

- [4] R.G. Zepp, D.G. Crosby (Eds.), *Aquatic and Surface Chemistry*, Lewis, Boca Raton, FL, 1994 (see, for example, Chapter 21, pp. 261–316).
- [5] A. Mills, C.E. Holland, R.H. Davies and D. Worsley, *J. Photochem. Photobiol., A: Chem.*, **83** (1994) 257–263.
- [6] L. Jacob, E. Oliveros, O. Legrini and A.M. Braun, in D.F. Ollis and H. Al-Ekabi (Eds.), *Photocatalytic Purification and Treatment of Water and Air*, Elsevier Science, 1993, pp. 511–532.
- [7] C. Tournaire, S. Croux, M.-T. Maurette, I. Beck, M. Hocquaux, A.M. Braun and E. Oliveros, *J. Photochem. Photobiol., B: Biol.*, **19** (1993) 205–215.
- [8] E. Fargin, M. Sergent, D. Mathieu and R. Phan-Tan-Luu, *Bio-Sciences*, **4** (1985) 77–82, and references cited therein.
- [9] G.E.P. Box, W.G. Hunter and J.S. Hunter, *Statistics for Experimenters: an Introduction to Design, Data Analysis and Model Building*, Wiley, New York, 1978.
- [10] A.I. Khuri and J.A. Cornell, in M. Dekker (Ed.), *Response Surfaces, Designs and Analyses*, ASQC Quality Press, New York, 1987.
- [11] D. Feneuille, D. Mathieu and R. Phan-Tan-Luu, *Méthodologie de la Recherche Expérimentale: Etude des Surfaces de Réponse*, L.P.R.A.I., Université d'Aix-Marseille, France, 1983.
- [12] D.H. Doehlert, *Appl. Stat.*, **19** (1970) 231–239.
- [13] D. Mathieu and R. Phan Tan Luu,  software (version 3.0), L.P.R.A.I., Université d'Aix-Marseille, France, 1995.
- [14] L. Amalric, C. Guillard and P. Pichat, *J. Photochem. Photobiol., A: Chem.*, **85** (1995) 257–262.
- [15] M. Trillas, J. Peral and X. Domènech, *Appl. Catal., B: Environmental*, **5** (1995) 377–387.
- [16] T.Y. Wei and C.C. Wan, *Photochem. Photobiol., A: Chem.*, **69** (1992) 241–249.
- [17] R.W. Matthews, *J. Catal.*, **111** (1988) 264–272.
- [18] V. Augugliaro, L. Palmisano, A. Sclafani, C. Minero and E. Pelizzetti, *Toxicol. Environ. Chem.*, **16** (1988) 89–109, and references cited therein.
- [19] A. Vidal, J. Herrero, M. Romero, B. Sanchez and M. Sanchez, *J. Photochem. Photobiol., A: Chem.*, **79** (1994) 213–219.
- [20] R.W. Matthews, *J. Phys. Chem.*, **91** (1987) 3328–3333.
- [21] C. Richard, *J. Photochem. Photobiol., A: Chem.*, **72** (1993) 179–182.
- [22] C. Richard and P. Boule, *New J. Chem.*, **18** (1994) 547–552.
- [23] A. Heller, J. Schwitzgebel, M.V. Pishko and J.G. Ekerdt, *Proc. Electrochem. Soc., (Water Purification by Photocatalytic, Photoelectrochemical and Electrochemical Processes)*, 1994, pp. 1–9.
- [24] H. Al-Ekabi, N. Serpone, E. Pelizzetti, C. Minero, M.A. Fox and R. Barton Draper, *Langmuir*, **5** (1989) 250–255.
- [25] R.W. Matthews, *Aust. J. Chem.*, **940** (1987) 667–675.
- [26] R.W. Matthews, *Solar Energy*, **38** (1987) 405–413.
- [27] C. Minero, *Solar Energy Mater. Solar Cells*, **38** (1995) 421–430.
- [28] D.F. Ollis and E. Pelizzetti, in N. Serpone and E. Pelizzetti (Eds.), *Photocatalysis, Fundamentals and Applications*, Wiley, New York, 1989, pp. 603–637.
- [29] C.S. Turchi and D.F. Ollis, *J. Catal.*, **119** (1989) 483–496.
- [30] T.Y. Wei and C.C. Wan, *Ind. Eng. Chem. Res.*, **30** (1991) 1293–1300.
- [31] J. Tseng and C.P. Huang, in D.W. Tedder and F.G. Pohland (Eds.), *Emerging Technologies in Hazardous Waste Management*, American Chemical Society, Washington, DC, 1990, Chapter 2, pp. 12–39.